Journal of
Materials Chemistry C

COMMUNICATION

View Article Online
View Journal | View Issue

Check for updates

Cite this: J. Mater. Chem. C, 2018, 6, 1328

Received 9th October 2017,
Accepted 18th December 2017

DOI: 10.1039/c7tc04587e

rsc.li/materials-c

A one-dimensional soft and color-programmable light-emitting device†

Zhitao Zhang,‡ Xiang Shi,‡ Huiqing Lou, Xunliang Cheng, Yifan Xu, Jing Zhang, Yiming Li, Lie Wang and Huisheng Peng *

A one-dimensional soft and color-programmable light-emitting device is developed by sandwiching an elastic light-emitting tube with two aligned carbon nanotube sheets. It can be stretched by over 200% without obvious fatigue in its illuminant property. Furthermore, its emission light can be controlled for different colors with tunable intensities that are independent of the observation angles. Based on its unique one-dimensional architecture, it can be continuously produced and assembled into various patterns or fabrics for large-scale application.

Light emission exists throughout nature.[1–6] For instance, halobios and insects, such as Phengodidae (commonly called railroad worm), can emit light from each of its body segments *via* paired photic organs for many important functions such as defence and courtship. Compared with the available man-made light-emitting devices, which are generally rigid and sometimes bendable, these natural light-emitting systems are soft and elastic, which are a key to solve the issues in the rapidly developing wearable electronics.[7–11] Wearable electronic devices with the function of light emission are required to stably attach onto and easily deform with irregular substrates;[12–15] these wearable light-emitting devices are highly desired for multi-disciplinary fields such as aerospace, transport, information technology, and healthcare.[16–20] For instance, light-emitting devices can be integrated with various wearable bioelectronics devices to monitor cardiac signals and temperature and body motion changes.[21,22] However, it is challenging to realize these soft light-emitting devices that mimic the promising paradigm in nature due to the difficulty of finding appropriate materials and designing comparable structures.

Herein, we fabricated a one-dimensional soft and color-programmable light-emitting device (SCLED) by sandwiching an elastic light-emitting tube with two aligned carbon nanotube (CNT) sheets. It can be stretched by over 200% without obvious fatigue in its illuminant property. Furthermore, its emission light can be controlled for different colors with tunable intensities that are independent of the observation angles. Based on its unique one-dimensional architecture, it can be continuously produced and assembled into various patterns or fabrics for large-scale application.

Fig. S1–S3 (ESI†) schematically demonstrate the fabrication process of the SCLED. First, aligned CNT sheets were continuously wrapped around a pre-stretched polymer fiber at a fixed angle of 45° to prepare the inner electrode, followed by coating a thin layer of silicone elastomer as a protecting layer. Herein, the aligned CNT sheet was directly drawn from a spinnable CNT array that was synthesized *via* chemical vapor deposition (Fig. S4, ESI†).[23,24] Subsequently, the inner electrode was inserted into an aligned CNT sheet-wrapped light-emitting tube to produce the SCLED. The image and structure of a lit SCLED are shown in Fig. 1a and b, respectively.

Fig. 2a and b show the scanning electron microscopy (SEM) images of the inner electrode with aligned CNT sheets closely

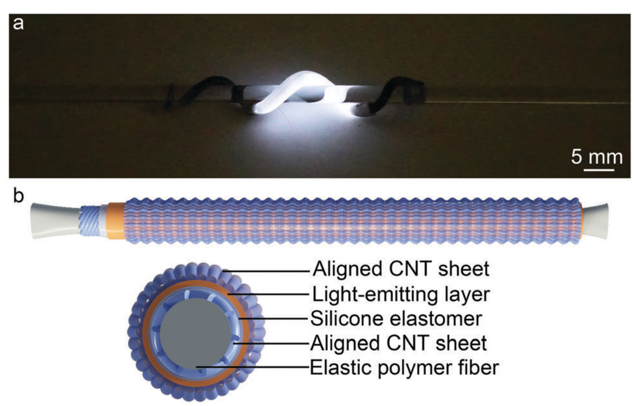

Fig. 1 (a) An image of the emitting SCLED being wrapped around a glass bar. (b) Schematic of the structure of the SCLED.

State Key Laboratory of Molecular Engineering of Polymers, Department of Macromolecular Science and Laboratory of Advanced Materials, Fudan University, Shanghai 200438, China. E-mail: penghs@fudan.edu.cn

† Electronic supplementary information (ESI) available. See DOI: 10.1039/c7tc04587e

‡ The first two authors contribute equally to this work.

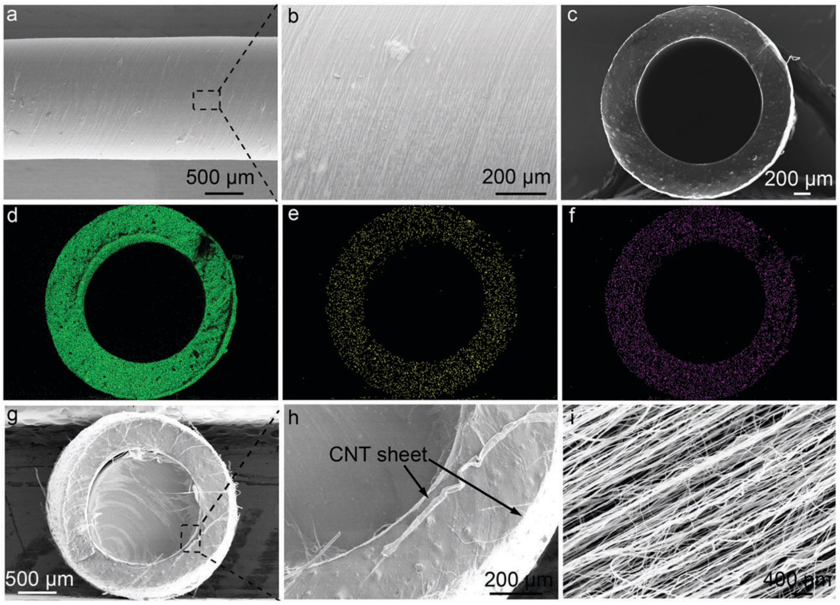

Fig. 2 SEM images of the SCLEDs. (a and b) Inner electrode at low and high magnifications, respectively. (c) Cross-sectional image of the light-emitting tube. (d–f) Dispersion of Si, Zn and S elements, respectively. (g and h) Cross-sectional images of the SCLED at low and high magnifications, respectively. (i) Outer CNT sheet electrode.

and uniformly wrapped around an elastic polymer fiber, which exhibit a stable contact between the aligned CNT sheet and polymer fiber due to van der Waals forces.[25–27] The helical angle of the wrapped aligned CNT sheet along the axial direction of the elastic polymer fiber remained almost unchanged by synchronizing the moving velocity of the translation stage and the precession velocity of the aligned CNT sheet. The thickness of the aligned CNT sheet layer was about 18 nm, and the wrapped aligned CNT layer thickness was accurately controlled by varying the width, helical angle and wrapping time of the wrapped aligned CNT sheet. Fig. S5 (ESI†) demonstrates the surface of the inner electrode after coating with a thin layer of silicone elastomer, which was mainly used to prevent the wrapped aligned CNT sheet from being damaged during the insertion process. The light-emitting tube possessed a uniform diameter with the ZnS phosphor powder well distributed in the silicone elastomer (Fig. 2c–f). The SEM image of the modified inner electrode after it was inserted into the light-emitting tube is shown in Fig. 2g and h and Fig. S6 (ESI†), which demonstrates a stable core–shell structure that is critical to improve the emitting performance. Meanwhile, the outer wrinkled CNT sheet electrode was also closely attached on the light-emitting tube to ensure effective light emission (Fig. 2i and Fig. S7, ESI†).

To increase the device performance, the preparation of an effective elastic electrode was a key step (Fig. 3a–c). The electrical properties of the inner electrode were first compared by wrapping aligned CNT sheets on the elastic polymer fiber with helical angles of 30°, 45° and 60°, while keeping the other conditions including the diameter of approximately 1670 μm for the elastic polymer fiber, pre-stretched strain of 100% and thickness of approximately 486 nm for the wrapped aligned CNT sheet nearly the same (Fig. S8, ESI†). Since the thickness of the wrapped aligned CNT sheet was the same, the electrical resistances were mainly compared based on contact resistances among the aligned CNTs which increased with an increase in the helical angle along the axial direction. As a result, the electrical resistances increased from 0.44 and 0.47 to 0.67 kΩ cm^{-1} with the increase in the wrapping helical angle from 30° and 45° to 60°, respectively. The changes in electrical resistance under stretching are further studied in Fig. 3d. The change ratios in resistance decreased from 7.34 and 1.30 to 1.27 with the increase in wrapping helical angle from 30° and 45° to 60° under the same strain of 200%, respectively. The changes in resistance are lower at higher wrapping helical angles owing to the higher initial electrical resistance. Considering the initial resistance and stretching stability, a wrapping helical angle of 45° is studied below if not otherwise specified.

The electrical resistance was also reduced from 2.41 to 0.47 kΩ cm^{-1} by increasing the thickness of the wrapped aligned CNT sheets from 97.2 to 486 nm (Fig. 3e). With a further increase in thickness, the electrical resistance remained nearly unchanged. Therefore, a CNT sheet thickness of 486 nm was explored. Fig. 3f and Fig. S9 (ESI†) demonstrate the cycling stability of the inner electrode during repeated stretching and releasing processes. The change in electrical resistance varied below 3% after stretching for 1000 cycles at a strain of 200%. For the outer electrode, the electrical resistances of the aligned CNT sheet (1 cm in width) decreased from 0.9 to 0.48 and 0.27 kΩ cm^{-1} with an increase in thicknesses from 18 and 36 to 54 nm, respectively. Notably, the optical transmittance decreased from 91% and 83% to 77% at a wavelength of 550 nm, respectively (Fig. 3g). As expected, stable stretchability was achieved due to the designed wrinkled structure of the CNT sheet (Fig. S10 and S11, ESI†).

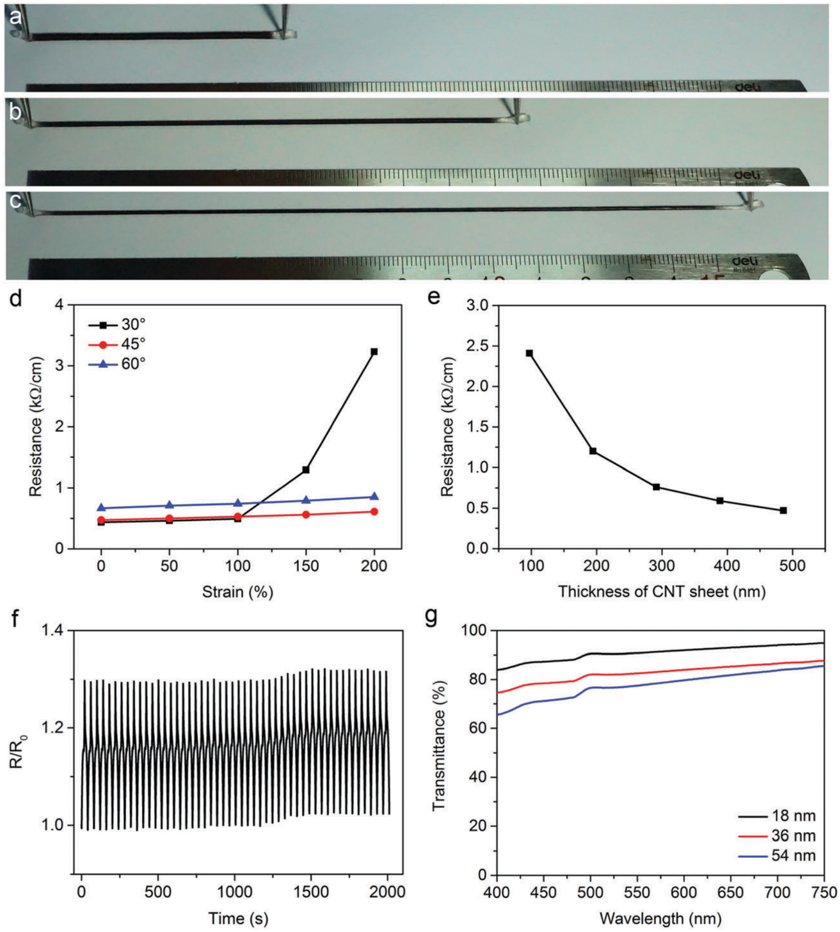

Fig. 3 Properties of the SCLED. (a–c) Photographs of the inner electrode before and after stretching by 100% and 200%, respectively. (d) Dependence of the electrical resistance of the inner electrode on strain. (e) Dependence of the electrical resistance of the inner electrode on the thickness of the wrapped aligned CNT sheet. (f) Dependence of the electrical resistance of the inner electrode on time under the repeated stretching and releasing process. (g) Dependence of the optical transmittance of the aligned CNT of the outer electrode on its thickness.

The SCLED can emit light under an alternating electrical field. The charge carriers under a strong alternating electrical field can be accelerated to excite the luminescent center to generate electron–hole pairs, which further recombine to emit light.[18] The luminance of the SCLED was first compared by increasing the thicknesses of the outer CNT sheet. As shown in Fig. 4a, the emission intensity decreased from 3.34 and 2.52 to 1.26 cd m^{-2} with an increase in thicknesses from 18 and 36 to 54 nm, respectively. Here, the transmission is dominant in the SCLED with the maximum emission intensity occurring at 18 nm which was subsequently used.

Fig. 4b demonstrates the luminance curve of the SCLED against an electrical field under frequencies of 1000 and 1500 Hz. The emission intensity increased from 0.36 to 14.48 cd m^{-2} with an increase in the electrical field from 2 to 6.4 V μm^{-1}, which is attributed to the enhanced excitation of the luminescent center. The relationship between luminance and voltage well matches the equation $L = L_0 \exp(-\beta/V^{1/2})$, where, L is the luminance, V is the applied voltage and L_0 and β are constants.[8,18] The emission intensity can also be controlled by changing the frequency of the applied voltage. A maximal value of 12.66 cd m^{-2} was achieved at 1500 Hz (Fig. 4c). At a lower frequency, the generated power was low; whereas, at a higher frequency, it is difficult for electrons and holes to combine. Due to its promising fiber shape, the SCLED can emit light in all directions with almost the same brightness (Fig. 4d).

The SCLED was highly stretchable, and was stretched as much as 200% (Fig. 4e). The luminance ratios after and before stretching increased from 1 to 3.8 with the increase in strain from 0 to 200% (Fig. 4f). The luminance change is mainly determined by three factors: (1) a decrease in the outer CNT sheet thickness contributes to a higher optical transmittance; (2) a decrease in the light-emitting layer thickness produces a larger electrical field; and (3) an increase in the light-emitting area generates a smaller density of light-emitting powder.[8] However, the increased optical transmittance and electrical field may play greater roles. The corresponding emission spectra are provided in Fig. 4g. This SCLED demonstrated good stretchability and maintained 97.5% of its emission intensity after stretching for 200 cycles at a strain of 200% with an increase in stretching speed up to 20% strain per second (Fig. 4h). This indicates its high flexibility with the variation in emission intensity maintained below 3% (Fig. S12, ESI†). The cross-sectional SEM images of the SCLEDs after

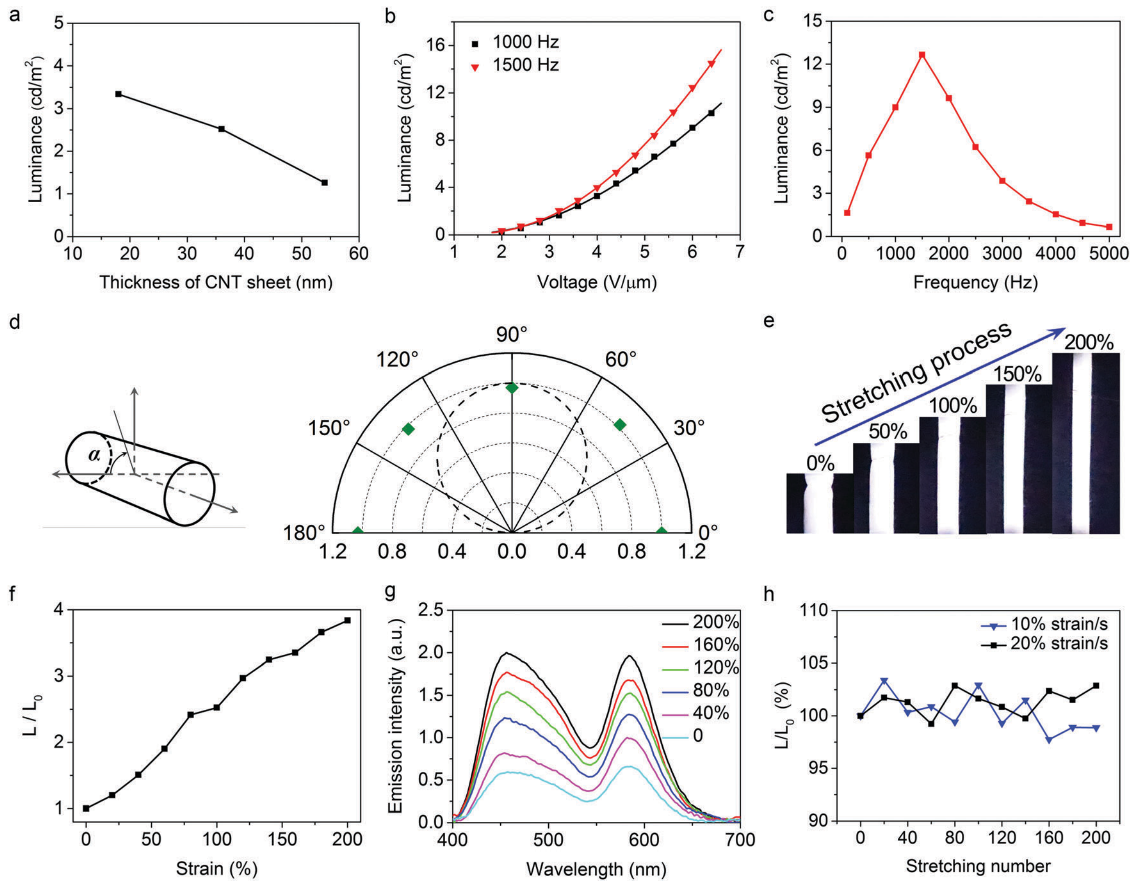

Fig. 4 (a) Dependence of luminance on thickness of the aligned CNT sheet. (b) Dependence of luminance on voltage. (c) Dependence of luminance on frequency under an electrical field of 6 V μm^{-1}. (d) Dependence of luminance on angle of the SCLED. L_0 and L correspond to the luminance measured at 0° and the other angle, respectively. (e) Photographs of the SCLED being stretched from 0%, 50%, 100% and 150% to 200%. (f) Dependence of luminance on strain. (g) Emission spectra at different strains. (h) Dependence of luminance on stretching number at different speeds. L_0 and L correspond to the luminance before and after stretching, respectively.

stretching at a strain of 200% for 200 cycles and bending for 1000 cycles were monitored, which do not indicate any obvious damage (Fig. S13, ESI†). The luminance and stretchability of our electroluminescent fiber and that of other reported stretchable electroluminescent devices were further compared, and the results are shown in Table S2 (ESI†).[28–37]

For practical applications, light-emitting devices are usually required to emit different colors and each color separately controlled. Thus, we designed an SCLED with different colored units sharing the inner electrode using ZnS powder which can emit different colors (Fig. 5a). As a result, it can form various patterns with different colors with the help of the circuit design (Fig. 5b). The photoluminescence spectra of the different colors of the ZnS powder are shown in Fig. S14 (ESI†). These SCLEDs can further be integrated onto the human body and selectively lit according to the requirement during use (Fig. 5c–g).

Although there are several studies on stretchable light-emitting devices, they mainly focus on planar structures, which is a bottleneck for many emerging promising fields such as wearable electronics. Herein, we have demonstrated the first example of stretchable fiber-shaped light-emitting devices that can be woven into elastic textiles (Fig. S15, ESI†). Furthermore, these stretchable light-emitting textiles solve the problem in planar light-emitting devices that are not permeable to air and water. They also open new application fields that remain difficult for planar light-emitting devices. For instance, they can be easily made into large-area displays for outdoor applications, which is difficult for their planar counterparts. They can also be conveniently and effectively integrated into clothes for next-generation portable and flexible microelectronic devices.

In summary, a new soft light-emitting SCLED is designed, which works even at a high speed of 20% strain per second and maintains above 97.5% of its emission intensity during stretching. Meanwhile, its unique one-dimensional shape enables the emission light to be independent of the viewing angle. Importantly, different units of color can be further integrated with each color for separate control. This work opens up a new direction for thee construction of soft optoelectronic and electronic devices.

Experimental

The preparation of the spinnable CNT array and inner electrode is provided in the ESI.†[38–40] The light-emitting tube with a

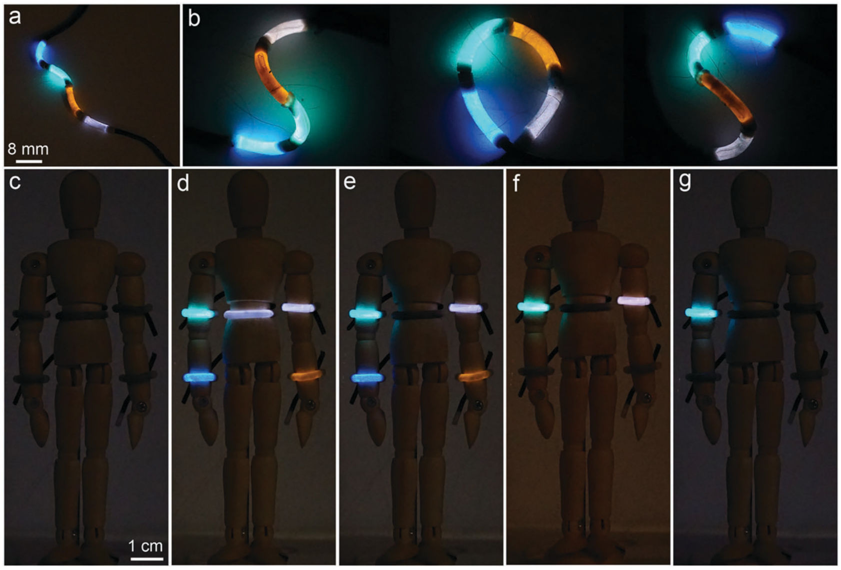

Fig. 5 An image of (a) an SCLED assembled from different light emission units, (b) SCLED deformed to form an 'SOS' pattern and (c–g) SCLEDs with different colors being selectively lit.

thickness of 350–400 μm was fabricated by injecting a light-emitting solution consisting of ZnS phosphor powder and silicone elastomers (weight ratio: 1/4) into a three-dimensionally printed, concentric cylinder mold, followed by curing at room temperature for 12 h and then drawing out of the mold. Subsequently, the aligned CNT sheet was scrolled onto the light-emitting tube at a pre-stretched strain of 200%, which was then released to the relaxing state. Finally, the pre-prepared inner electrode was inserted into this modified light-emitting tube to produce the SCLED. The multicolor SCLEDs were produced in a similar way by integrating different color light-emitting tubes onto the same inner electrode.

Conflicts of interest

There are no conflicts to declare.

Acknowledgements

This work was supported by MOST (2016YFA0203302), NSFC (21634003, 51573027, 51403038, 51673043, 21604012) and STCSM (16JC1400702, 15XD1500400, 15JC1490200).

References

1 C. H. Contag and M. H. Bachmann, *Annu. Rev. Biomed. Eng.*, 2002, **4**, 235.
2 S. H. D. Haddock, M. A. Moline and J. F. Case, *Annu. Rev. Mar. Sci.*, 2009, **2**, 443.
3 V. R. Viviani and E. J. H. Bechara, *Ann. Entomol. Soc. Am.*, 1997, **90**, 389.
4 T. Nakatsu, S. Ichiyama, J. Hiratake, A. Saldanha, N. Kobashi, K. Sakata and H. Kato, *Nature*, 2006, **440**, 372.
5 Y. Ando, K. Niwa, N. Yamada, T. Enomoto, T. Irie, H. Kubota, Y. Ohmiya and H. Akiyama, *Nat. Photonics*, 2008, **2**, 44.
6 Y. Ohta and Y. Hatada, *J. Biochem.*, 2006, **140**, 475.
7 H. L. Filiatrault, G. C. Porteous, R. S. Carmichael, G. J. E. Davidson and T. B. Carmichael, *Adv. Mater.*, 2012, **24**, 2673.
8 J. Wang, C. Yan, G. Cai, M. Cui, A. Lee-Sie Eh and P. See Lee, *Adv. Mater.*, 2016, **28**, 4490.
9 D. Yin, J. Feng, N.-R. Jiang, R. Ma, Y.-F. Liu and H.-B. Sun, *ACS Appl. Mater. Interfaces*, 2016, **8**, 31166.
10 J. Liang, L. Li, K. Tong, Z. Ren, W. Hu, X. Niu, Y. Chen and Q. Pei, *ACS Nano*, 2014, **8**, 1590.
11 H.-H. Chou, A. Nguyen, A. Chortos, J. W. F. To, C. Lu, J. Mei, T. Kurosawa, W.-G. Bae, J. B. H. Tok and Z. Bao, *Nat. Commun.*, 2015, **6**, 8011.
12 H. Yang, C. R. Lightner and L. Dong, *ACS Nano*, 2012, **6**, 622.
13 T. Sekitani, H. Nakajima, H. Maeda, T. Fukushima, T. Aida, K. Hata and T. Someya, *Nat. Mater.*, 2009, **8**, 494.
14 M. S. White, M. Kaltenbrunner, E. D. Glowacki, K. Gutnichenko, G. Kettlgruber, I. Graz, S. Aazou, C. Ulbricht, D. A. M. Egbe, M. C. Miron, Z. Major, M. C. Scharber, T. Sekitani, T. Someya, S. Bauer and N. S. Sariciftci, *Nat. Photonics*, 2013, **7**, 811.
15 J. Liang, L. Li, X. Niu, Z. Yu and Q. Pei, *Nat. Photonics*, 2013, **7**, 817.
16 S. Kwon, W. Kim, H. Kim, S. Choi, B.-C. Park, S.-H. Kang and K. C. Choi, *Adv. Electron. Mater.*, 2015, **1**, 1500103.
17 V. Vohra, U. Giovanella, R. Tubino, H. Murata and C. Botta, *ACS Nano*, 2011, **5**, 5572.
18 C. Larson, B. Peele, S. Li, S. Robinson, M. Totaro, L. Beccai, B. Mazzolai and R. Shepherd, *Science*, 2016, **351**, 1071.
19 Z. Zhang, K. Guo, Y. Li, X. Li, G. Guan, H. Li, Y. Luo, F. Zhao, Q. Zhang, B. Wei, Q. Pei and H. Peng, *Nat. Photonics*, 2015, **9**, 233.

20 Z. Zhang, Q. Zhang, K. Guo, Y. Li, X. Li, L. Wang, Y. Luo, H. Li, Y. Zhang, G. Guan, B. Wei, X. Zhu and H. Peng, *J. Mater. Chem. C*, 2015, **3**, 5621.
21 J. H. Koo, S. Jeong, H. J. Shim, D. Son, J. Kim, D. C. Kim, S. Choi, J.-I. Hong and D.-H. Kim, *ACS Nano*, 2017, **11**, 10032.
22 J. Kim, H. J. Shim, J. Yang, M. K. Choi, D. C. Kim, J. Kim, T. Hyeon and D.-H. Kim, *Adv. Mater.*, 2017, **29**, 1700217.
23 Z. Zhang, X. Chen, P. Chen, G. Guan, L. Qiu, H. Lin, Z. Yang, W. Bai, Y. Luo and H. Peng, *Adv. Mater.*, 2014, **26**, 466.
24 Z. Zhang, J. Deng, X. Li, Z. Yang, S. He, X. Chen, G. Guan, J. Ren and H. Peng, *Adv. Mater.*, 2015, **27**, 356.
25 D. Tasis, N. Tagmatarchis, A. Bianco and M. Prato, *Chem. Rev.*, 2006, **106**, 1105.
26 M. Moniruzzaman and K. I. Winey, *Macromolecules*, 2006, **39**, 5194.
27 Z. Wu, Z. Chen, X. Du, J. M. Logan, J. Sippel, M. Nikolou, K. Kamaras, J. R. Reynolds, D. B. Tanner, A. F. Hebard and A. G. Rinzler, *Science*, 2004, **305**, 1273.
28 C. Larson, B. Peele, S. Li, S. Robinson, M. Totaro, L. Beccai, B. Mazzolai and R. Shepherd, *Science*, 2016, **351**, 1071.
29 J. X. Wang, C. Y. Yan, G. F. Cai, M. Q. Cui, A. L. S. Eh and P. S. Lee, *Adv. Mater.*, 2016, **28**, 4490.
30 F. Stauffer and K. Tybrandt, *Adv. Mater.*, 2016, **28**, 7200.
31 S. Li, B. N. Peele, C. M. Larson, H. C. Zhao and R. F. Shepherd, *Adv. Mater.*, 2016, **28**, 9770.
32 J. X. Wang, C. Y. Yan, K. J. Chee and P. S. Lee, *Adv. Mater.*, 2015, **27**, 2876.
33 C. H. Yang, B. H. Chen, J. X. Zhou, Y. M. Chen and Z. G. Suo, *Adv. Mater.*, 2016, **28**, 4480.
34 Z. Yu, X. Niu, Z. Liu and Q. Pei, *Adv. Mater.*, 2011, **23**, 3989.
35 J. J. Liang, L. Li, X. F. Niu, Z. B. Yu and Q. B. Pei, *Nat. Photonics*, 2013, **7**, 817.
36 M. S. White, M. Kaltenbrunner, E. D. Glowacki, K. Gutnichenko, G. Kettlgruber, I. Graz, S. Aazou, C. Ulbricht, D. A. M. Egbe, M. C. Miron, Z. Major, M. C. Scharber, T. Sekitani, T. Someya, S. Bauer and N. S. Sariciftci, *Nat. Photonics*, 2013, **7**, 811.
37 S. G. R. Bade, X. Shan, H. Phong Tran, J. Li, T. Geske, L. Cai, Q. Pei, C. Wang and Z. Yu, *Adv. Mater.*, 2017, **29**, 1607053.
38 R. Li, X. Xiang, X. Tong, J. Zou and Q. Li, *Adv. Mater.*, 2015, **27**, 3831.
39 C. P. Huynh and S. C. Hawkins, *Carbon*, 2010, **48**, 1105.
40 X. Lepró, M. D. Lima and R. H. Baughman, *Carbon*, 2010, **48**, 3621.